Tetragonality and Properties of $Ba(Zr_xTi_{1-x})O_3$ Ceramics Determined Using the Rietveld Method

HONG-HSIN HUANG, HSIN-HSIUNG CHIU, NAN-CHUNG WU, and MOO-CHING WANG

$Ba(Zr_xTi_{1-x})O_3$ (x = 0, 0.05, 0.1, and 0.15, BZT for short) has been prepared using the solid solution reaction from $BaTiO_3$ (BT) and $BaZrO_3$ (BZ). For transmission electron microscopy (TEM) analysis, the cubic phase of BZT coexists with the tetragonal one in the $Ba(Zr_{0.15}Ti_{0.85})O_3$ ceramics. Its structure of ceramics has been estimated using the Rietveld and Cohen methods. The effect of $BaZrO_3$ content on the tetragonality of BZT and its relation to a dielectric constant have been studied, and it is found that the tetragonality approaches 1 as the BZ content is increased, while simultaneously the Curie temperature of BZT decreases at a rate of 4.66 °C per mole pct BZ. The average grain size was sensitive to the BZ content, and the P_r could be enhanced at room temperature.

DOI: 10.1007/s11661-008-9622-2

I. INTRODUCTION

FOR some time now, high-permittivity (high-k) materials have been widely used for dielectrics in commercial capacitor application, and materials with large switchable spontaneous polarization, or ferroelectrics, have also been closely studied in the pursuit of low-voltage, high-speed, nonvolatile memory. $BaTiO_3$ (BT) is a high-k perovskite dielectric, which is under extensive investigation as an alternative material for use at the 1 Gbit density and beyond.[1] A high-k modifier, such as $BaZrO_3$ (BZ), may be alloyed into $BaTiO_3$ to form a solid solution, which can be used to obtain a broad phase transition region. This results in the Curie temperature decreasing; therefore, a high dielectric constant device could be obtained, which can be used over a wide temperature range.[2] In addition, it has been found that with the partial substitution of Zr at Ti sites in $BaTiO_3$, the paraelectric to ferroelectric phase transition (T_c) is shifted to a lower temperature, making the rhombohedral to orthorhombic and orthorhombic to tetragonal phase transition temperature increase.[3,4]

The effect on dielectric properties of adding BZ to BT to form a $Ba(Zr,Ti)O_3$ (BZT) solid solution has been reported by Dixit *et al.*[4] and Jiang *et al.*[5] The BZT ceramics are usually used for making capacitors; therefore, most studies focus on the temperature dependence of the dielectric constant, the nature of phase transition, and the relaxor behavior of these ceramics. The effect of the changed microstructure on its physical properties has been studied using the Cohen method,[6] which is fragmented for multiphase structure analysis. So far, the coexistence of multiphase and the limitations of X-ray diffraction (XRD) have not been discussed in detail,[4,5] a vacancy in research that we hope to fill. Traditionally, it has been difficult to distinguish between the tetragonal and cubic forms, because there is no splitting of the peaks, but we have found that this problem may be overcome using the Rietveld method, which is a structure-precise technique for powder diffraction analysis.[7–9] In the present article, the tetragonality and properties of $Ba(Zr_xTi_{1-x})O_3$ ceramics were studied using XRD, scanning electron microscopy, transmission electron microscopy (TEM), electron diffraction, impendence analysis, and the Rietveld and Cohen methods. The purpose of present research is to investigate the effect of BZ content on (1) the structure, (2) the tetragonality, and (3) the dielectric properties of BZT ceramics.

II. EXPERIMENT

The BT and BZ ceramics were separately prepared *via* the method of solid-state reaction. The starting materials, $BaCO_3$ (99.9 pct, Katayama, Japan), TiO_2 (99.9 pct, Katayama), and ZrO_2 (99.9 pct, Showa, Japan) powders with a stoichiometric composition of $BaTiO_3$ and $BaZrO_3$, were ball milled with deionized water for 10 hours and then calcined at 1200 °C for 2 hours to form the single-phase BT and BZ powders. The BT and BZ powders were blended into several compositions according to the stoichiometric composition of $BaZr_xTi_{1-x}O_3$, with x = 0, 0.05, 0.10, and 0.15. After drying, 1 wt pct PVA was added and a disk 12 mm in diameter and 0.8-mm thickness was formed under a pressure of 3.9 MPa. Finally, these samples were sintered at 1350 °C for 1.5 hours in a furnace and then

HONG-HSIN HUANG, Associate Professor, is with the Department of Electrical Engineering and Department of Chemical and Materials Engineering, Cheng Shiu University, Kaohsiung 83347, Taiwan, R.O.C. HSIN-HSIUNG CHIU, Master, and NAN-CHUNG WU, Professor, are with the Department of Materials Science and Engineering, National Cheng Kung University, Tainan 70101, Taiwan, R.O.C. MOO-CHING WANG, Professor, is with the Faculty of Fragrance and Cosmetics, Kaohsiung Medical University, Kaohsiung 80708, Taiwan, R.O.C. Contact e-mail: mcwang@kmu.edu.tw
Manuscript submitted January 3, 2008.
Article published online October 25, 2008

cooled to room temperature. The structure of the samples was analyzed by X-ray diffraction (D/Max V, Rigaku, Tokyo, Japan), Cu K_α (λ = 1.54056 Å) with a scanning rate ranging from 0.25 to 0.5 deg/min at a step of 0.02 deg. These XRD patterns were calculated by the Rietveld method to obtain the structure model with the least deviation. The microstructure of BZT was analyzed by TEM (model 3010, JEOL*), and the Ag-pasted samples were used as electrodes after being sintered at 780 °C for 2 hours and stabilized for 30 days. The dielectric constant of BZT was measured at temperatures ranging from −40 °C to 140 °C using an impedance analyzer (HP4263A, Yakogawa Hewlett Packard, Tokyo, Japan) with an applied AC voltage of 1 V and a frequency of 1 kHz. The dielectric constant (ε_r) was calculated using Eq. [1]:

*JEOL is a trademark of Japan Electron Optics Ltd., Tokyo.

$$\varepsilon_r = \frac{Cd}{\varepsilon_0 A} \quad [1]$$

where C is the capacitance, d the sample's thickness (m), A the area of Ag electrode (m^2), and ε_0 the permittivity of the free space ($8.854 \cdot 10^{-12}$ F/m). The hysteresis loop was measured at 10 kHz and 5 V using a modified Sawyer–Tower circuit.

III. RESULTS AND DISCUSSION

A. *The Structure of BZT Ceramics*

The structure of the BT alloyed with various BZ contents was analyzed by XRD, and these results are shown in Figure 1. They reveal that the forked peaks of pure BT gradually merge as the BZ content is increased, which suggests that the tetragolity of ceramics gradually transforms toward the cubic one as the BZ content is increased. The BZT structure was found to fully change from a tetragonal to a cubic structure, possessing a lattice constant of 4.052 Å when the addition of BZ content is higher than 25 mol pct, as reported by Hennings *et al.*[10] In addition, Figure 1 also shows that the forked peaks not only become close to each other, but that the diffraction angle also decreases as the BZ content is raised, as shown in the embedded figure. The substitution of Ti^{4+} [$R(Ti^{4+})$ = 0.745 Å] by larger Zr^{4+} [$R(Zr^{4+})$ = 0.86 Å] will increase the d spacing of BZT and cause the diffraction peaks to shift toward a lower angle.[4] Neirman[11] has also pointed out that both lattice parameters c and a of the $(Ba_{0.75}Sr_{0.25})(Zr_xTi_{1-x})O_3$ solid solution increase with the increase in Zr content; however, the ratio of c/a decreases. Moreover, when the Zr content is higher than 10 mol pct, the lattice constant increases in direct proportion to the increasing Zr content.[11]

The XRD pattern of $Ba(Zr_{0.15}Ti_{0.85})O_3$ and the Rietveld fitting curve were shown in Figure 2, which is a typical result relative to $Ba(Zr_{0.05}Ti_{0.95})O_3$ and $Ba(Zr_{0.10}Ti_{0.90})O_3$. In Figure 2, the weighted profile R factor, R_{wp}, is 17.92 pct, and the goodness-of-fit indicator, s, is 1.3, which demonstrates that this simulation is reliable. A satisfactory agreement was observed between the measured and calculated pattern of BZT.

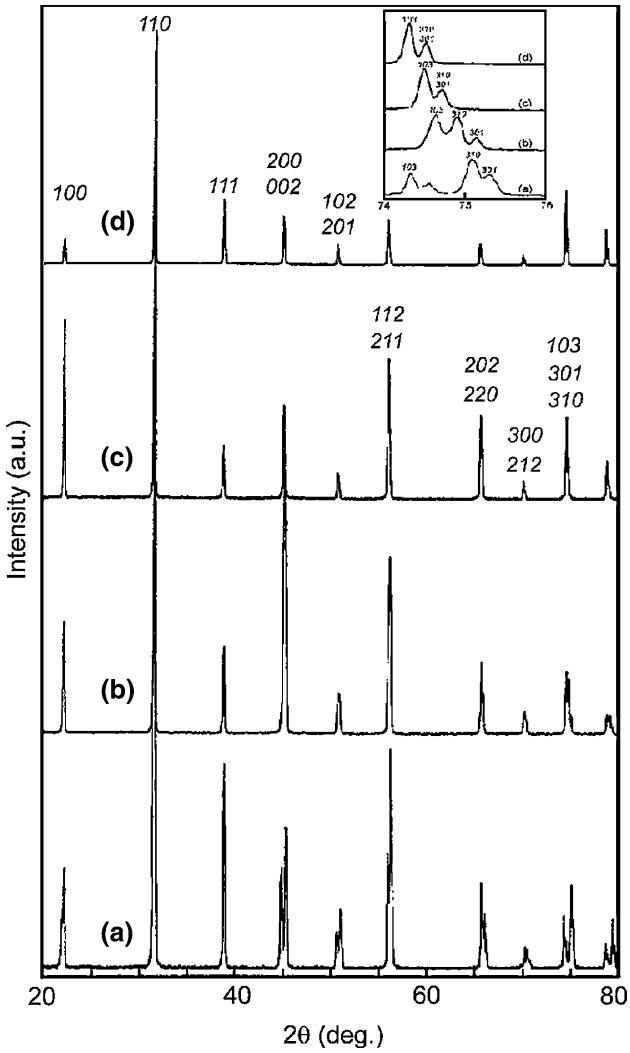

Fig. 1—XRD patterns of BT with various BZ contents of (*a*) 0, (*b*) 5, (*c*) 10, and (*d*) 15 mol pct.

In the present study, the XRD results reveal that although the lattice parameter a increases with the increasing Zr content, it also approaches the lattice parameter c. It would be useful to determine whether the cubic phase exists simultaneously with the tetragonal one, resulting in the lattice constant shift. However, the existence of the cubic phase of ceramics cannot be clearly determined using XRD analysis, as the X-rays are diffracted by the d spacing of the lattice of either the tetragonal or cubic phases. Consequently, microstructure analysis is necessary to verify the existence of the cubic phase. The bright-field (BF) and dark-field (DF) of the BZT ceramic are shown in Figures 3(a) and (b), denoting grains precipitated in the matrix. The selected area electron diffraction (SAED) analyses of the $Ba(Zr_{0.15}Ti_{0.85})O_3$ crystal marked as A and B are also shown in Figures 3(c) and (d), respectively. The indexing

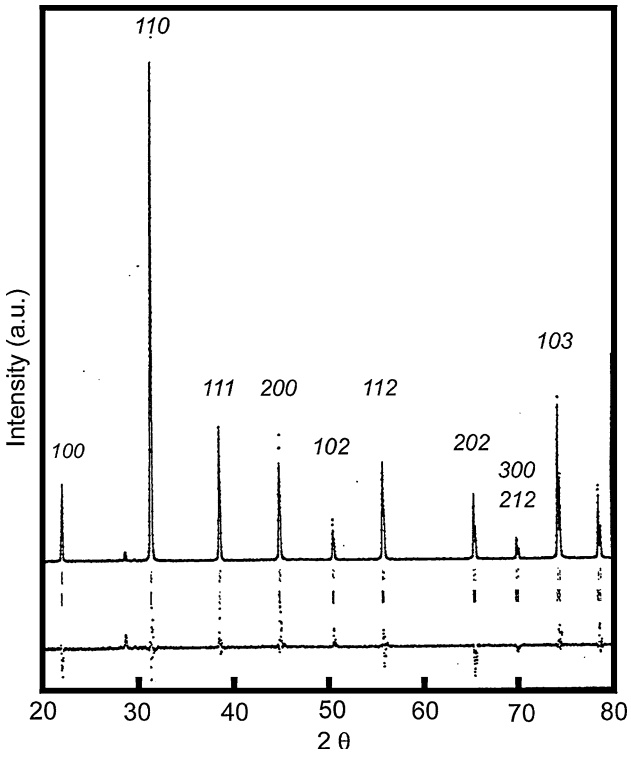

Fig. 2—XRD pattern and Rieveld fitting curve of $Ba(Ti_{0.85}Zr_{0.15})O_3$.

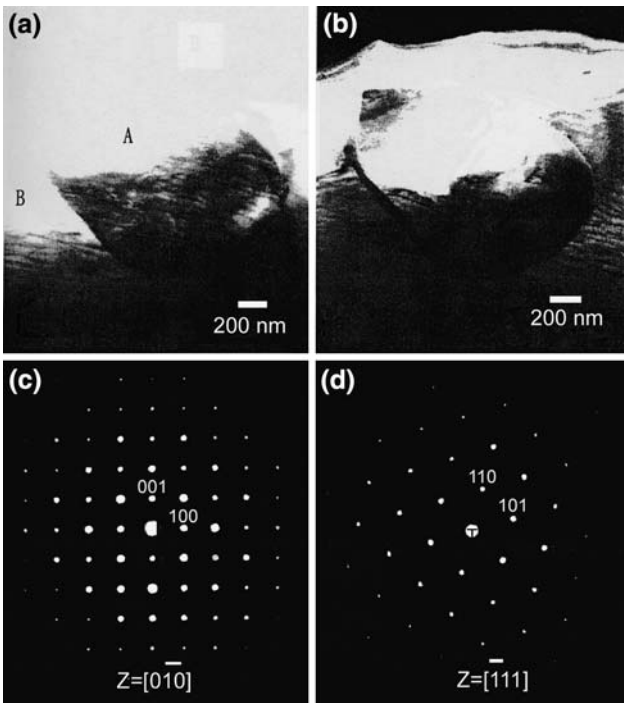

Fig. 3—TEM analysis of $Ba(Ti_{0.85}Zr_{0.15})O_3$: (*a*) BF, (*b*) DF, (*c*) SAED of A grain, and (*d*) SAED of B grain.

of the SAED patterns reveals that A is a cubic phase and matrix B is a tetragonal phase, which demonstrates that the BZ content induces cubic phase formation in the matrix of the tetragonal one; this demonstrates the coexistence of both tetragonal and cubic phases in the BZT ceramics. From this, it may be deduced that numerous false conclusions may be arrived at if the ceramic is considered as a single phase.

Table I. Comparison of the Standard Formation Energies of $BaTiO_3$ and $BaZrO_3$

Parameter	$BaTiO_3$[12]	$BaZrO_3$[13]
Gibbs free energy (kJ/mole)	−1572.3	−125.56 ± 2

Hennings *et al.*[10] reported that a diffuse phase transition observed near the Curie temperature of BZT ceramics is shown to be caused by coexisting ferroelectric and paraelectric phases, which can be described by a normal distribution of Curie temperatures. In addition, a small difference in the Curie temperature was observed; therefore, two reasons were deduced: a mechanical stress distribution in the material or variation in chemical composition caused by sintering process.[10] For a BZT solid solution formation, the substitution of Ti^{4+} by Zr^{4+} results in mechanical stress formed in the BZT ceramics; consequently, a lattice constant shift was detected. Table I lists the comparison of standard formation energy of $BaTiO_3$[12] and $BaZrO_3$[13] ceramics. According to Maxwell's relation of $(\partial S/\partial V)_T = (\partial P/\partial T)_V$, the mixture of BT and BZ results in the increase in entropy of BZT ceramics, where S, V, P, and T are entropy, volume, pressure, and temperature.[14] This increase of entropy gives the decrement of Gibbs free energy: $G = G^0 - T\Delta S$, where G^0 is the Gibbs free energy before mixing.[14] Therefore, the coexistence of cubic and tetragonal phases of BZT is possible. Owing to the limitations of XRD, the simulation of the Rietveld method should prove to be a powerful tool both for determining the existence of the cubic phase and for reducing inaccuracies in the lattice determination.

The ratio of the cubic/tetragonal phase and its lattice parameters are of utmost concern for the present study. The Rietveld method has been used to simulate the precise structure of the tetragonal and cubic phases, and in order to obtain the exact lattice constants of BZT, the XRD patterns were measured at a very slow scanning rate (0.25 to 0.5 deg/min by a step of 0.02 deg) and calibrated with Si powders. The lattice parameters of BZT using the Cohen method thus obtained are shown in Figure 4(a), which indicates that the lattice parameter a increases toward the c value as the BZ content is increased, and both the c and a values increase even further when the Zr content is higher than 10 mol pct, a result not consistent with the corresponding TEM examination. Therefore, the Rietveld analysis for the multiphase system must be employed to obtain a precise structure simulation. (The simulation results for BZT ceramics with various BZ contents are listed in Table II.) The reliability index of the weighted profile R factor, R_{wp}, values of 17.45, 15.95, and 17.92 pct were obtained, which means the simulation is reliable; in addition, the goodness-of-fit indicator, s, values of 1.4, 1.1, and 1.3 were obtained, which means a good fitting is accomplished. As Table II shows, the cubic phase in the BZT

solid solution is 36.73 pct for 5 mol pct BZ. Furthermore, when the BZ content is increased to 15 mol pct, the cubic phase becomes 64.9 pct. The content of the cubic phase increases along with the increasing BZ content, although the increment decreases as the BZ level rises. Moreover, the density of the BZT solid solution decreases as the Zr content increases, as seen in Table II. Souma and Ohtaki[15] have demonstrated that the density of the bulk crystal estimated by the Rietveld method is very close to the measured value. The higher the density, the lower the vacancy or void in the ceramics, resulting in both a higher dielectric constant and a lower Curie temperature. The dielectric behavior should be predictable, based on a combination of the existence of the cubic phase, the c/a ration of the tetragonal phase, and the theoretical density for ceramics with various BZ contents.

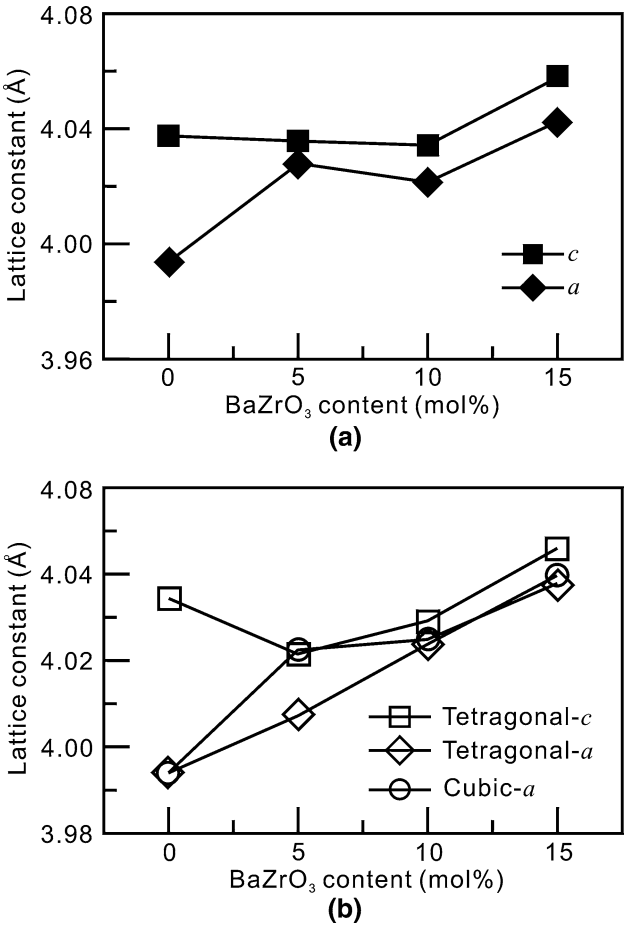

Fig. 4—Dependence of lattice constant on BZ content estimated by the (*a*) Cohen method and (*b*) Rietveld method.

The BZT lattice parameters obtained by the Rietveld method are shown in Figure 4(b), where it can be seen that the lattice parameter c decreases from 4.0345 to 4.0214 Å when the BZ content is increased from 0 to 5 mol pct, and then increases from 4.0214 to 4.0457 Å when the BZ content is further increased from 5 to 15 mol pct. However, the lattice parameter a linearly increases from 3.9943 to 4.0394 Å as the BZ content is increased from 0 to 15 mol pct. It should be noted that both lattice parameters a and c continuously approach each other. This phenomenon is caused by Ti^{4+} replacing Zr^{4+} at the B site of the perovskite structure, creating an increased radius of the B site and thus a larger increase of the a value than of the c value. As this is occurring, the distance between the B sites in the polarization axis also decreases, resulting also in a decrease in the Curie temperature.[16]

B. *Relation between the Tetragonality and the BZ Content of BZT Ceramics*

Figure 5 illustrates the relation between the tetragonality and the BZ content of BZT ceramics. It reveals that the tetragonality of BZT dramatically decreases (from 1.0101 to 1.0035) as the BZ content is increased from 0 to 5 mol pct, but then only slightly decreases (from 1.0035 to 1.0016) when the BZ content is increased from 5 to 15 mol pct. It should be also noted that it has a minimum value of 1.0019 at 5 pct BZ content when estimated using the Cohen method. Arlt[17] has reported that the formation of the ferroelectric domain fundamentally reduces the homogeneous stress within a given grain. As this happens, the inhomogeneous stress mainly forms in the grain boundaries, where a large internal stress occurs. When the tetragonality decreases, it leads to reduced internal stress due to the formation of 90 deg ferroelectric domains. For this reason, the dielectric constant increases and the

Table II. Phase Ratios and Lattice Constants of Various BZT Sintered at 1350 °C for 1.5 Hours and Refined by the Rietveld Method

Parameters	$Ba(Zr_{0.05}Ti_{0.95})O_3$	$Ba(Zr_{0.10}Ti_{0.90})O_3$	$Ba(Zr_{0.15}Ti_{0.85})O_3$
Cubic : Tetragonal Phase	0.3673 : 0.6327	0.5623 : 0.4377	0.6487 : 0.3513
a-Value of cubic phase (Å)	4.0223 ± 0.0002	4.0247 ± 0.0003	4.0377 ± 0.0001
a-Value of tetragonal phase (Å)	4.0072 ± 0.0002	4.0235 ± 0.0002	4.0394 ± 0.0002
c-Value of tetragonal phase (Å)	4.0214 ± 0.0002	4.0291 ± 0.0005	4.0457 ± 0.0003
Theoretical Density (g/cm^3)*	6.0525	6.0471	6.0294
R_{wp}**	17.45	15.95	17.92
$s^{\dagger}$	1.4	1.1	1.3

*Theoretical density: total weight divided by total volume.
**R_{wp}: weighted profile R factor.
†s: goodness-of-fit indicator.

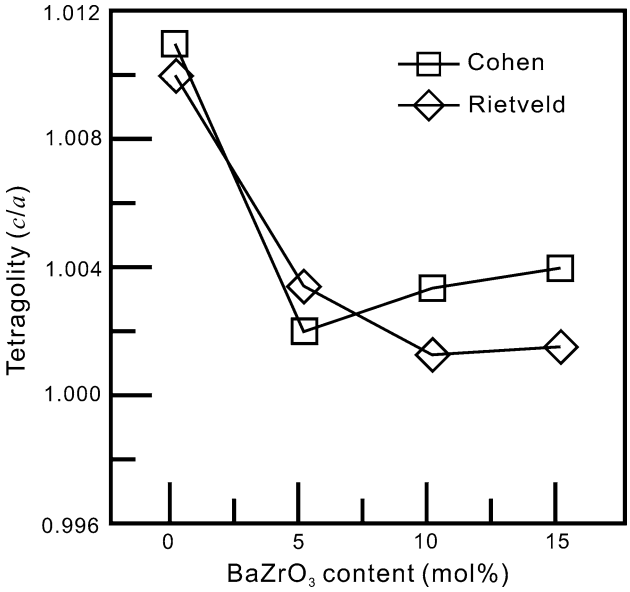

Fig. 5—Dependence of BZT tetragolity on BZ content.

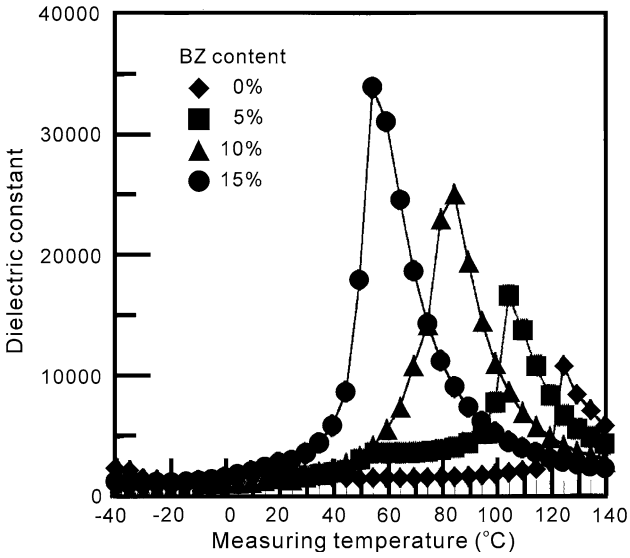

Fig. 6—Dependence of BZT dielectric constant on measuring temperature as a function of BZ content.

c/a ratio decreases to constrain spontaneous polarization. By increasing the BZ content, the tetragonality of the tetragonal phase approaches 1, and the values of a and c of the tetragonal phase come close to the a value of the cubic phase.

C. *Dependence of the Dielectric Properties, Microstructure, and BZ Content of BZT Ceramics*

Figure 6 shows the dependence of the dielectric constant of BZT on the measuring temperature as a function of BZ content. This figure indicates that as the BZ content increases from 0 to 15 mol pct, the Curie temperature simultaneously decreases from 125 °C to 56 °C. The reduction in the Curie temperature due to the BZ content is 4.66 °C per mol pct BZ. The relation between the Curie temperature and BZ content is shown in Figure 7. Masuno *et al.*[18] have pointed out that the dependence of the Curie temperature on the BZ content consistently shows a slope of −5 °C/mol pct. The results of the present study are consistent with the values obtained by Masuno *et al.*;[18] however, the effect of the amount of cubic phase on the dielectric properties needs further investigation. The largest Curie temperature decrease with Zr content is considered to be due to a decrease in the pseudo-Jahn–Teller effect,[19] where the interaction between phonons and electrons results in a B-site atom shift in a BO_6 octahedral structure. The interaction is reduced because the increased Zr content and the overlap of the $d\pi$ and $p\pi$ orbits cause the Curie temperature to decrease.[20]

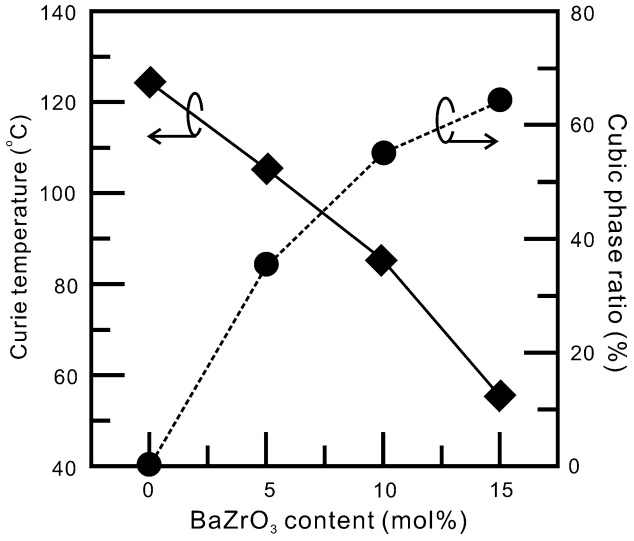

Fig. 7—Dependences of Curie temperature and cubic phase ration on BZ content.

The dependence of the Curie temperature and the cubic phase ratio of BZT on the BZ content are shown in Figure 7. It is found that the Curie temperature decreases and the cubic phase ratio increases as the BZ content is increased. From this, it may be deduced that the decrease in the Curie temperature is simultaneously caused by the tetragonality shift and the cubic phase formation.

The effect of BZ content on the grain size of BZT is shown in Figure 8, in which it can be seen that a more dense bulk is observable in all the BZT ceramics and that the average grain size increases as the BZ content rises. Dixit *et al.*[4] revealed that the morphology feature appears to be quite sensitive to the BZ content for a sol-gel process; they concluded that BZ enhances the grain growth of BZT. As illustrated in Figure 7, the cubic phase content increases along with the BZ content; thus, the observed phenomenon by Dixit *et al.*,[4] in the morphological features changes with BZ contents, could be deduced to be related to the phase formation. Dixit *et al.*[4] also reported that beyond 20 mol pct Zr contents, the grain sizes of BZT become quite uniform.

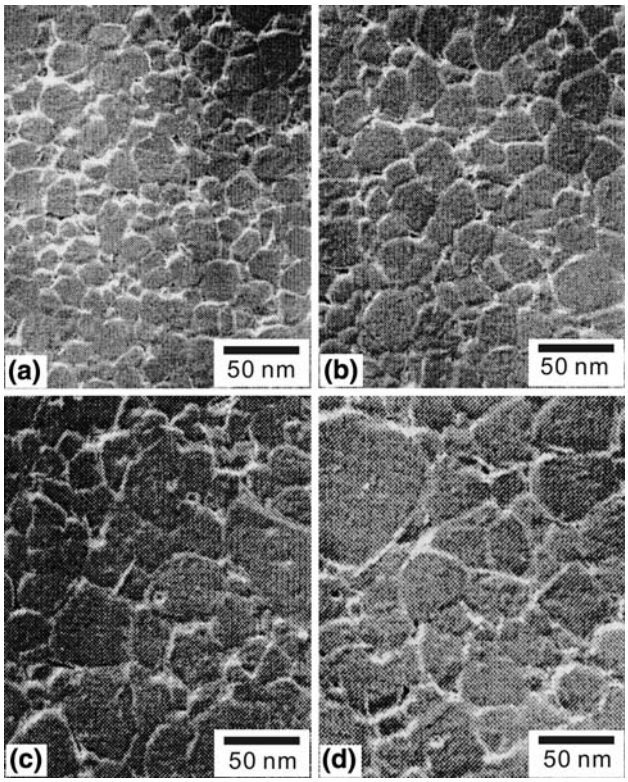

Fig. 8—Micrograph of BZT with various BZ contents of (*a*) 0, (*b*) 5, (*c*) 10, and (*d*) 15 mol pct.

The similar trend was found in cubic phase content, as shown in Figure 7, and tetragonality, as shown in Figure 5, which levels off when BZ content is higher than 15 pct.

As can be seen in Figure 6, the Curie temperature of BZT with various BZ contents is higher than 50 °C, meaning that the ceramics possess ferroelectric properties at room temperature. The hysteresis loop (*P vs E*) of BT and $Ba(Zr_{0.15}Ti_{0.85})O_3$ are shown in Figure 9, where it can be seen that the P_r may be enhanced by the addition of BZ. Yu *et al.*[3] report that the P_r of $Ba(Zr_{0.15}Ti_{0.85})O_3$ is 0.08 $\mu C/cm^2$, which is quit smaller, although its Curie temperature is close to room temperature. The profiles of *P vs E* are related to the crystalline structure of ceramics at room temperature.[3,4] The higher the BZ content, the higher the cubic phase ratio. It could be deduced from this that the dielectric properties can be further enhanced by increasing the tetragonal phase ratio in the ceramics.

IV. CONCLUSIONS

The tetragonality of BZT decreases to 1 as the BZ content is increased. For 5 mol pct BZ content, the lattice parameter *c* of BZT decreases but *a* increases, resulting in a dramatic decrease of tetragonality. In addition, this research found that there is a minimum *c*-axis value of 4.0214 Å. Moreover, both lattice parameters *a* and *c* increase when the BZ content is higher than 5 mol pct. When the BZ content increases, not only does the tetragonality of BZT approach 1 but the cubic phase also coexists in the tetragonal phase matrix. The phase ratio of the cubic phase increases from 36.73 to 64.87 pct when the BZ content is increased from 5 to 15 mol pct, although the increment decreases. It is found that the Curie temperature decreases with an increasing BZ content. The decrement of the Curie temperature is 4.66 °C per mol pct BZ. The average grain size is sensitive to the BZ content, and the P_r can be enhanced at room temperature.

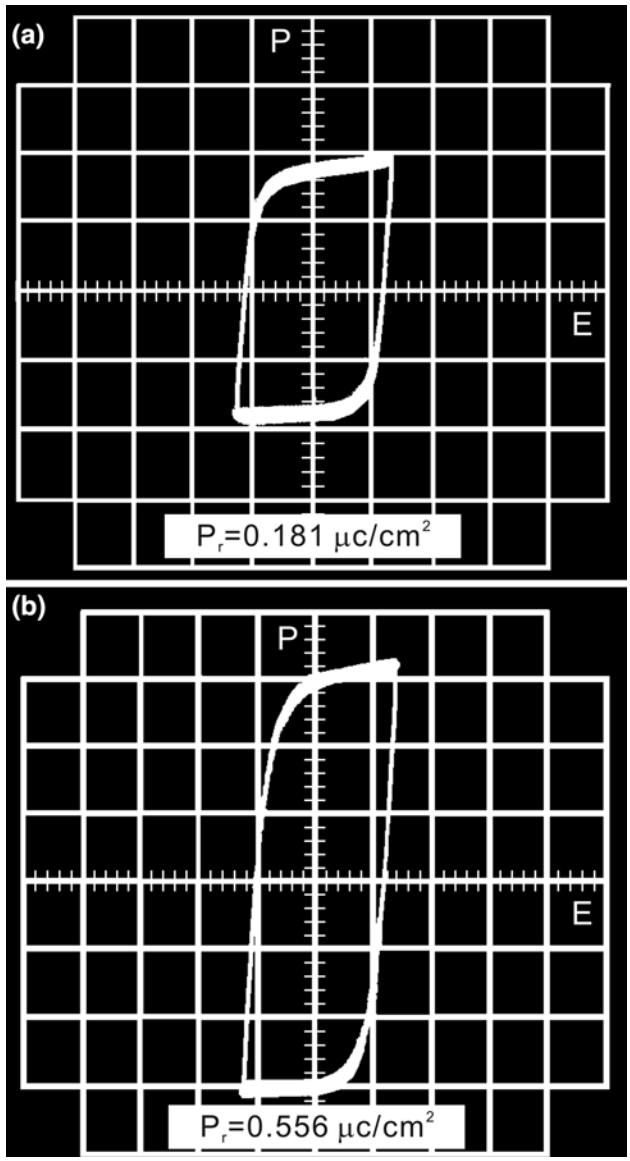

Fig. 9—Hyteresis loop of (*a*) $BaTiO_3$ and (*b*) $Ba(Zr_{0.15}Ti_{0.85})O_3$.

ACKNOWLEDGMENTS

This work was supported by the National Science Council, Taiwan, under Contract No. 94-2216-E-151-001, which is gratefully acknowledged. The authors

sincerely thank Professor M.P. Hung for the manuscript discussion and Messrs. J.M. Chen and S.Y. Yao for their assistance with XRD and TEM.

REFERENCES

1. R.E. Jones, Jr., P. Zurcher, P. Chu, D.J. Taylor, Y.T. Lii, B. Jiang, P.D. Maniar, and S.J. Gillespie: *Microelectron. Eng.*, 1995, vol. 29, pp. 3–10.
2. A.-M. Azad and S. Subramaniam: *Mater. Res. Bull.*, 2002, vol. 37, pp. 11–21.
3. Z. Yu, C. Ang, R. Guo, and A.S. Bhalla: *J. Appl. Phys.*, 2002, vol. 92, pp. 1489–93.
4. A. Dixit, S.B. Majumder, P.S. Dobal, R.S. Katiyar, and A.S. Bhalla: *Thin Solid Films*, 2004, vols. 447–448, pp. 284–88.
5. X.P. Jiang, M. Zeng, H.L.W. Chan, and C.L. Choy: *Mater. Sci. Eng. A*, 2006, vol. 198, pp. 438–40.
6. B.D. Cullity: *Elements of X-ray Diffraction*, 2nd ed., Addison Wesley, Massachusetts, MA, 1978, pp. 363–68.
7. M.L. Moreira, S.A. Pianaro, A.V.C. Andrade, and A.J. Zara: *Mater. Charact.*, 2006, vol. 57, pp. 193–98.
8. A.F. Gualtieri, A. Viani, and C. Montanari: *Cement Concrete Res.*, 2006, vol. 36, pp. 401–06.
9. D.A. Clemente, E. Lucchini, S. Meriani, and N. Furlan: *J. Euro. Ceram. Soc.*, 2005, vol. 25, pp. 1863–76.
10. D. Hennings, A. Schnell, and G. Simon: *J. Am. Ceram. Soc.*, 1982, vol. 65, pp. 539–44.
11. S.M. Neirman: *J. Mater. Sci.*, 1988, vol. 23, pp. 3973–80.
12. X.Y. Wang, S.W. Lu, B.I. Lee, and L.A. Mann: *Mater. Res. Bull.*, 2000, vol. 35, pp. 2555–63.
13. K.T. Jacob and Y. Waseda: *Metall. Mater. Trans. B*, 1995, vol. 26B, pp. 775–81.
14. K. Kamishima, Y. Nagashima, and K. Kakizaki: *J. Phys. Soc. Jpn.*, 2008, vol. 77, 064801 pp. 1–4.
15. T. Souma and M. Ohtaki: *J. Alloys Compd.*, 2006, vol. 413, pp. 289–97.
16. V.V. Kirillov and V.A. Isupov: *Ferroelectrics*, 1973, vol. 5, pp. 3–9.
17. G. Arlt: *Ferroelectrics*, 1990, vol. 104, pp. 217–27.
18. K. Masuno, T. Murakami, and S. Waku: *Ferroelectrics*, 1972, vol. 3, pp. 315–19.
19. K. Kristoffel and P. Konsin: *Phys. Status Solidi*, 1967, vol. 21, p. K39.
20. I.B. Bersuker: *Phys. Lett.*, 1966, vol. 20, pp. 589–90.